Lab on a Chip

PAPER

View Article Online
View Journal | View Issue

Cite this: *Lab Chip*, 2020, **20**, 4456

How electrospray potentials can disrupt droplet microfluidics and how to prevent this†

Andrea J. Peretzki,[a] Sabine Schmidt,[b] Elias Flachowsky,[a] Anish Das,[a] Renata F. Gerhardt[a] and Detlev Belder *[a]

Received 16th September 2020,
Accepted 8th October 2020

DOI: 10.1039/d0lc00936a

rsc.li/loc

A pressure-resistant microfluidic glass chip that integrates a packed-bed HPLC column, a droplet generator and a monolithic electrospray emitter is presented. This approach enables a seamless coupling of chip-HPLC and droplet microfluidics with ESI-MS detection. For the electrical contacting of the emitter, an electrode was integrated into the channel, which reaches up to the emitter tip. The incidental finding that under certain circumstances, the electrospray potential can strongly disturb the droplet microfluidics by electrowetting, was investigated in detail. Strategies to avoid this are evaluated and include electrical shielding and/or chip layouts, where the droplet generator is positioned at a long distance from the emitter.

Introduction

Microfluidic systems find a wide range of applications in chemistry, biology, and medicine. In particular, droplet microfluidics, where femto- to microliter samples are encapsulated by an immiscible carrier fluid, is used for various applications including high-throughput screenings in chemical synthesis or bioassays.[1–6] An important aspect to make droplet microfluidics a valuable tool for versatile applications is the choice of a suitable detection technology. For this purpose, mass spectrometry is becoming increasingly popular as it is nearly universally usable and does not require labeling steps. For online analyses of aqueous droplets, electrospray ionization (ESI) is the dominant ionization method,[7] while offline matrix-assisted laser desorption/ionization mass spectrometry (MALDI-MS) is also used.[8–10] To enable electrospray ionization of a segmented flow, an electrical potential must be applied between the droplet phase and the MS inlet. In droplet microfluidics, usually only the disperse polar, mostly aqueous phase is electrically conductive, so it is necessary to consider how the electrical potential can be transferred from the emitter to the droplets. The easiest way to realize this is to implement an electrically conductive capillary emitter which is compatible with capillary-based droplet systems[11–17] as well as with polymer chip devices. In particular, when using popular polydimethylsiloxane (PDMS) devices,[18–22] the insertion of a conductive emitter such as steel capillaries into the flexible chip material is very easy to do.

PDMS devices are perfect choices for various applications as respective chips can be straightforwardly manufactured by applying soft lithography. In addition, the hydrophobic nature of the surface perfectly matches the requirement for most applications. Namely, the channel walls should be hydrophobic to provide good wetting properties for the continuous oil phase and to prevent interactions of the droplet phase with the surface. Nevertheless, elastomeric PDMS chips also have some disadvantages. An important one is the limited burst pressure, which prevents their use for microfluidic processes operating at high pressures, such as chip-based high performance liquid chromatography (HPLC). Accordingly, in our earlier work on the integration of chip-HPLC and droplet microfluidics,[23,24] we chose glass as the device material.

Such a combination of chip-HPLC and droplet microfluidics can be regarded as a microfluidic analogue to common fraction collection in traditional HPLC. This can be seamlessly realized on a chip if the column eluate is fractionated into small segments by the introduction of an immiscible phase through a micromachined droplet generator directly after the HPLC column.[23–26] The eluate is thus segmented into droplets that are spaced apart by the oil flow, preventing peak dispersion and promoting mixing within the droplets. The latter effect is particularly attractive to facilitate post-column reactions in microfluidics. This approach combines two prominent areas of microfluidics, the chip-based separation techniques and the field of droplet microfluidics.[27–31] This now gives chip-HPLC access to the toolbox of droplet microfluidics for the targeted control of processes on the

[a] *Institute of Analytical Chemistry, Leipzig University, Johannisallee 29, D-04103 Leipzig, Germany. E-mail: belder@uni-leipzig.de*
[b] *Center for Biotechnology and Biomedicine, Molecular Biological-Biochemical Processing Technology, Leipzig University, Deutscher Platz 5, D-04103 Leipzig, Germany*

† Electronic supplementary information (ESI) available: Flow and MS conditions, additional videos, measurements, chip designs, discussion. See DOI: 10.1039/d0lc00936a

nano- to picoliter scale, such as droplet splitting, aggregation, sorting, extraction or reagent addition.[32–35]

In all previous proof-of-concept studies on the combination of chip-HPLC and droplet microfluidics, however, only fluorescence detection was used, which significantly limits the range of applications. One motivation for the current study was to realize mass spectrometric detection to read the chemical contents of individual droplets of the dispersed column eluate.

We chose glass as chip substrates of choice to seamlessly integrate HPLC separation, droplet microfluidics, and electrospray ionisation on a single pressure-resistant device. In contrast to elastomeric PDMS systems, which are widely used in droplet microfluidics, it is, however, not possible to simply plug in a conductive electrospray emitter such as a steel capillary into a rigid glass chip.

The most elegant approach for electrospray emitters in glass chips is their monolithic integration,[36–38] which was also chosen for the current work. The typical approaches for electrical contacting of the emitter in microfluidic systems made from glass, *e.g. via* a conductive liquid phase or *via* an appropriate make-up flow functionality, do not work if the carrier liquid is not electrically conductive, as is usually the case in droplet microfluidics. An alternative is to use integrated metal electrodes.[39] However, when high electric potentials are applied close to the droplet phase, it must be taken into account that the corresponding electric fields can also disturb droplet formation and stability.

The influence of electric fields on droplets is often used intentionally for active and precise droplet manipulations in microchannels, such as electrically controlled droplet generation,[40,41] droplet fusion,[42,43] droplet deflection,[44] droplet extraction,[45,46] and especially droplet sorting.[47–49] In digital microfluidics, discrete droplets are manipulated by applying electrical potentials between electrodes,[50] and the respective electrowetting effects are used to move, split, or unite the droplets.[51–53]

Although the detection of droplets in ESI-MS has been presented several times, only Wink *et al.* and Schirmer *et al.* reported that the applied electrospray potential can affect droplet formation or movement.[22,54] In our current study, we observed that this effect is much more pronounced in glass chips with monolithically integrated ESI emitters and embedded electrodes compared to our previous work using PDMS devices.[21,22] In the present contribution, this phenomenon is explored and solutions are provided, which were key to finally enable chip-HPLC-droplet/MS hyphenation for the first time.

Experimental

Chemicals and materials

Analytical standard high-performance liquid chromatography (HPLC) grade acetonitrile, ethanol, methanol, and 2-propanol were purchased from VWR International GmbH. High-purity water was provided by a Smart2Pure purifying system (18.2 MΩ cm, TKA Wasseraufbereitungssysteme GmbH). Ammonium acetate, caffeine, choline chloride, L-lysine, 7-amino-4-methylcoumarin, perfluorodecalin, and trichloro-(1*H*,1*H*,2*H*,2*H*-perfluorooctyl)silane were purchased from Sigma-Aldrich GmbH. Krytox 157FS was purchased from DuPont de Nemours GmbH. Microscopic slides (soda-lime, 76 mm × 26 mm) were purchased from Carl Roth GmbH. The photoresist AZ 1518, developer AZ 351B, chromium etchant TechniEtch Cr01, and HF solution BOE 7 : 1 ($HF:NH_4F$ = 12.5 : 87.5%) were purchased from MicroChemicals GmbH. The photoresist AR-N 4340 for the structuring of the electrode was purchased from Allresist GmbH. The chromium target was purchased from MaTeck GmbH (99.95%) and the platinum target from Junker Edelmetalle (99.99%). For shielding experiments, common adhesive copper tape was used (6 mm Behr Bircher Cellpack BBC AG).

Initial chip design

The mobile phase and the analytes were introduced into the chip using a steel clamp, connecting a polyether ether ketone (PEEK) capillary with the microfluidic system *via* powder blasted inlet holes. The adjoining HPLC column channel was confined by narrowings at both ends with integrated photo-polymerized porous frits retaining the column particles. The subsequent droplet generator consisted of a common T-junction. The droplet channel ended in an emitter ground to a tip with an integrated sputtered platinum electrode. The channels were 30 μm deep and 200 μm wide (width of narrowings 75 μm).

Chip fabrication

All microfluidic chips were fabricated in-house by photolithographic processing followed by wet etching and high-temperature bonding. Commercially available microscopic slides made of soda-lime glass (Carl Roth GmbH) were used as substrates. The microfluidic channels were hydrophobized using a 1 vol% solution of trichloro(1*H*,1*H*,2*H*,2*H*-perfluorooctyl)silane as described earlier.[23] The chromatographic column was generated by an established slurry packing procedure[23,24,55] using 3 μm ProntoSil C18 SH as a stationary phase material (Bischoff Analysentechnik und -geräte GmbH). The packing channel was sealed afterward by photopolymerization. To manufacture the emitter, first, a tip was roughly sawn (Proxxon Micromot 230/E with a diamond cutting disc) and broken off and then ground using a grinding machine (Proxxon TG 125/E equipped with sandpaper Bosch C470, rotating grinding discs equipped with sandpaper Klingspor P2500) and finally hydrophobized.[38] The platinum electrodes were sputtered onto the structured bottom or lid slides. Before coating, the glass substrates were cleaned in an ultrasonic bath (P360D, Martin Walter Ultraschalltechnik AG) with acetone and 2-propanol. Subsequently, they were cleaned in piranha solution as well as in hydrofluoric acid, finally rinsed with ultrapure water, and cured at 200 °C. After cooling to room

temperature, the photoresist AR-N 4340 (Allresist GmbH) with a thickness of 3 μm was spin-coated at 1000 rpm (Primus SB15, SSE GmbH). The resist was exposed through a film mask in a mask aligner (SUSS MicroTec GmbH) with a wavelength spectrum of 350–405 nm. After puddle development, the substrate surface was partially exposed for coating. The electrodes were applied by sputtering with a BAE 250 system (BALZERS GmbH). For this purpose, a 50 nm thick adhesion promoter layer of chromium was applied with a 2″ target (99.95%, MaTeck GmbH) at 3.7×10^{-3} mbar and a target–substrate distance of 150 mm. For the platinum layer, a 2″ target (99.99%, Junker GmbH) was used to apply a 500 nm thick layer. After coating, the excess photoresist with platinum was dissolved in acetone.

For chip layout 1 (Fig. 1), the channels were first structured, then the electrodes were sputtered onto them and bonded to a cover plate with holes. The width of the electrode in the area of the droplet channel was 135 μm. In layout 2 (Fig. 6), the electrodes were sputtered onto the lid glass slides and the connection holes were integrated and bonded to the structured glass bottom. This offered the advantage that the lids with the electrodes could be prefabricated independently of the channel design. The width of the electrode in the area of the droplet channel was 1.14 mm.

For the indium tin oxide (ITO) sputtering, the chips were cleaned with acetone and 2-propanol. A 4″ target (90 : 10 wt%; EVOCHEM GmbH) and the sputtering system CREAMET 500 (CREAVAC GmbH) were used for coating. At a pressure of 4.0×10^{-3} mbar, a working distance of 150 mm and a sputtering power of 250/85 W (RF/DC), a layer thickness of approx. 500 nm was achieved with a sputtering time of 20 min. To avoid exposing the chips to thermal stress, which could lead to breakage, the ITO layer was not annealed.

Instrument setup and detection

MS experiments: instead of the commercial ESI source, the microfluidic chip was placed in front of the MS orifice on an xyz micromanipulator. Opposite the emitter tip, an electrically contacted metal plate was installed a few millimeters away, serving as a counter electrode. The MS inlet was located orthogonally to this arrangement. The distances between the MS inlet, the emitter tip, and the counter electrode were optimized to achieve stable signals and high signal intensity. Two different MS systems were used: an LCMS-2010A quadrupole mass spectrometer from Shimadzu for the experiments with applied potential on-chip and a 6150 LC/MS system from Agilent for potential on the MS inlet and the chip on ground. The MS conditions for all measurements are listed in Table S1.† For power supply, a bipolar 1-channel (HCN 35-35000, FuG Elektronik GmbH) or 4-channel (HCV 40M-10000, FuG Elektronik GmbH) high-voltage source was used.

For microscopic investigations, the microfluidic chip was placed on the xy stage of an epifluorescence microscope iX-70 (Olympus Europa SE & Co. KG) and an electrically contacted metal plate was placed a few millimeters away from the tip, mimicking the MS orifice. A 5× objective (CP-Achromat, Carl Zeiss AG) was used for photographic pictures and videos taken by a consumer camera (Canon EOS 750D).

A syringe pump system including a base module (B100-01A) and high pressure (B207-01A) and low pressure (B002-02D) modules provided fluidics and monitoring of the backpressure using the software QMixElements 2.6 (Cetoni GmbH). The polar mobile phase was moved by the high-pressure pump equipped with a 2.5 mL stainless steel syringe. The analyte was added continuously to the column inlet of the microfluidic chip *via* a 6-port valve with a 100 μL sample loop (Rheodyne Model 7125, IDEX Health & Science LLC.). The sample injection, for elution *via* the column of the microfluidic chip, was performed externally through a 4-port nano-injection valve with a 5 nL sample loop (VICI AG). All high-pressure devices were connected *via* PEEK capillaries (360 μm OD × 75 μm ID, VICI AG). The non-polar continuous phase perfluorodecalin (PFD) was introduced using low-pressure pumps with 250 μL glass syringes (ILS GmbH) *via* polytetrafluoroethylene (PTFE) tubing (1.58 mm OD × 0.3 mm ID, Supleco) with LuerTight fitting (P-835 IDEX Corp.). The MS experiments were performed without the addition of a surfactant to facilitate the ionization of the analytes and to avoid contamination of the MS. Standard PTFE sealing tape was attached at the hydrophobized emitter tip to drain the oil off and avoid disturbing the spray.

Safety considerations

Hydrofluoric acid is acutely toxic and leads to severe symptoms of poisoning or even death, even in the case of small areas of corroded skin. Appropriate protective clothing including gloves and eye and face protection is mandatory.

Beware of high voltages. Handle with extreme care. Only touch the setup when the voltage is off. Instruments that must be operated during measurements must be provided with a ground cable.

Results and discussion

In our previous work, we demonstrated the successful coupling of chip-HPLC and droplet microfluidics in soda-lime glass chips, which integrates two powerful microfluidic techniques in one device.[23,24] This allows complex mixtures to be analyzed and processed on a single chip. By segmenting the column eluate into a droplet phase, a wide variety of process operations from the world of droplet microfluidics can now be applied downstream of the HPLC column. While we used fluorescence detection for that first proof-of-concept studies, the motivation for the current contribution was to develop an approach for online mass spectrometric detection. This should considerably expand the application range of this new technology. Building upon our extensive experience in MS detection in glass chips,[56–58] such as chip-based HPLC/MS,[38] we decided to develop a new chip layout, which includes a monolithically integrated glass emitter for electrospraying individual droplets

of the segmented chip-HPLC eluate. A prerequisite for inducing an electrospray at the emitter tip is the electrical contacting of the liquid to be sprayed. In our previous work on droplet-chip/MS coupling the chip was equipped with an electrically conductive steel capillary as ESI-emitter.[21,22] While the manual insertion of such a capillary into the microfluidic chip works well with elastomeric PDMS chips, it is not reasonably applicable with rigid glass chips. For inducing an electrospray at a monolithically integrated glass chip-emitter, we often used in earlier work the approach to simply contact the liquid outside the chip, *e.g.* before it enters the chip or *via* make-up flow channels.[59] This is, however, not compatible with droplet microfluidics, where in most cases, the continuous oil phase is electrically non-conductive. Another approach for the electrical contacting of the emitter is the chip integration of electrodes, *e.g.*, by sputtering, which we also realized in our earlier reports on chip-HPLC.[39] For this to work also with droplet microfluidics, a conductive channel coating must be integrated, which covers all the way to the front of the emitter to electrically contact the droplet there. We have developed a respective chip layout, which includes such an integrated platinum electrode as well as a packed HPLC column, a droplet generator, and a droplet channel. A schematic drawing of the whole droplet-chip/MS setup, the chip layout, together with an annotated photograph of a chip is shown in Fig. 1. A sample is injected onto the chip column, where the LC separation takes place. The eluate is then dispersed in the droplet generator into segmented droplets, which are carried by the continuous oil phase to the ESI emitter, which incorporates a sputtered Pt electrode. From there, the droplets are electrosprayed and enter the mass spectrometer while the oil is drained away. The microfluidic chip is placed in front of the orifice of the mass spectrometer using a home-built interface consisting of an xyz-translation stage and a counter electrode as described in previous work on coupling droplet PDMS chips with MS.[21,22] The electrospray is generated by a potential difference between the emitter and the counter electrode consisting of an electrically contacted metal plate. This arrangement was positioned vertically in front of the MS orifice and allows independent adjustment of the distances and potential differences between the chip, the counter electrode, and the MS and additionally minimizes the contamination of the mass spectrometer with the oil.[21] This arrangement, in which the ESI emitter does not spray directly into the MS orifice, could lead to ion loss and thus to reduced sensitivity. This was studied in comparative experiments. These indicated that the detection of stable and regular droplet traces works with both chip-MS arrangement, where the emitter tip was directed towards the MS orifice and with the MS placed orthogonally to the chip emitter (see Fig. S1†). Also, the analyte signal shows a better signal shape in the orthogonal arrangement. With direct infusion, more spikes are visible, which could be attributed to a higher oil entry into the MS. The desolvation of the ESI droplets could be further improved by using commercial sprayers with sheath gas.[12,14,16,60] This approach, however, requires long transfer capillaries to attach the chip to the ESI sprayer of the mass spectrometer.

In our initial studies to perform MS detection with our HPLC-droplet-ESI chip, pure acetonitrile (ACN) was used as an HPLC eluent. This results in ACN droplets segmented by the oil phase perfluorodecalin (PFD). By applying a potential of +2.5 kV at the chip electrode, an intermitting electrospray was generated as expected. Caffeine (200 μM) was added to the eluent as a test analyte to monitor the droplet ionization process by the mass spectrometer. An intermittent trace of signals at a frequency of 1.2 Hz was detected by the MS, as shown in Fig. 2a. This shows that the droplets are formed regularly so that the content of each droplet is read by the mass spectrometer.

The variation of the intensity of the droplet peaks with a relative standard deviation of 15% around the mean value of 5.0×10^6 counts can be attributed to the relatively low measuring frequency of 5.6 Hz in scan mode. The respective experimental conditions, such as flow rates and MS conditions, are given in Table S1.†

After this first successful proof of concept, a 10 mM purely aqueous ammonium acetate buffer at pH 7.4 was chosen as

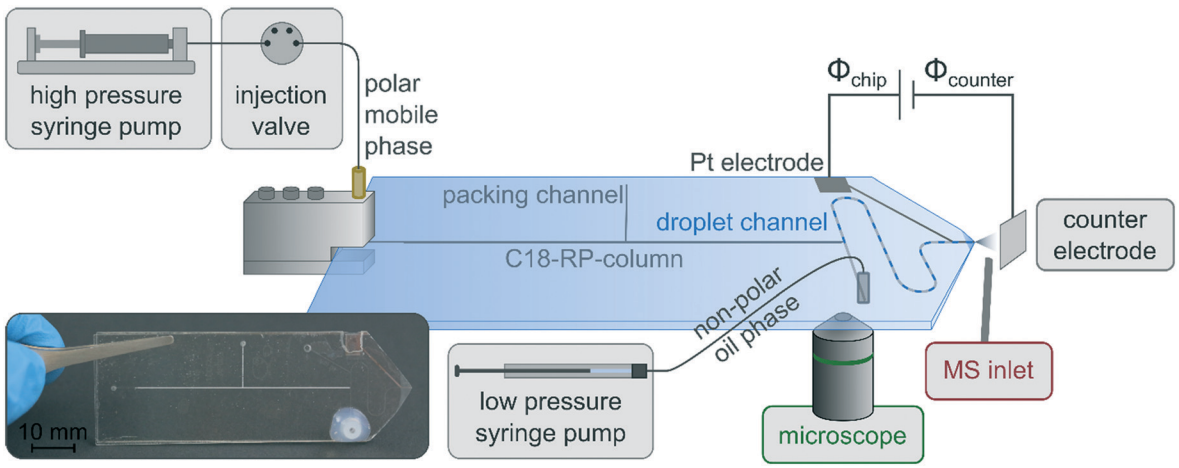

Fig. 1 Schematic drawing of the chip layout and the experimental setup for microscopic (green) or MS studies (red). The photo shows a glass chip with a packed column, droplet channel and ground ESI emitter with an integrated platinum electrode.

the mobile phase. To our astonishment, much worse results were achieved with dispersed water droplets although water is the more common medium in droplet microfluidics. Compared to the previous experiments with pure ACN droplets, the MS trace of the aqueous droplets was rather irregular and showed strongly fluctuating intensities, as shown in Fig. 2b.

In order to study this unexpected behaviour in more detail, analogous chip electrospray experiments were conducted on an inverted optical microscope using a counter electrode to mimic the MS inlet. By light microscopic imaging of the droplets in the channel, it became evident that droplet formation worked reliably well when no voltage was applied to the chip emitter. A respective microscopic image of the section where the HPLC column joins the oil channel and the droplet generation takes place is shown in Fig. 3a.

While droplet generation worked well without applied potentials, the droplet process was massively disrupted soon after the high voltage at the chip integrated platinum electrode was switched on. The droplet formation became erratic, and wetting of the channel walls was observed as well as downstream droplet merging in an uncontrolled manner, as shown in Fig. 3b. A respective video of the process is given in the ESI† (Video S1).

Additional experiments with different potential values showed that the droplets were already affected at much lower potentials where no electrospray had been formed yet. At a potential of 0.75 kV the droplets were already slightly deformed, and above 0.85 kV the potential induced an intense droplet deformation, and they were also torn apart. At least 1.7 kV was required to induce the electrospray process. The data of these set of experiments are summarised in Table S2.†

As the high potential applied to the platinum electrode in contact with the segmented liquid flow obviously disrupted the water droplet flow, we tried another approach to generate the required electric field between the electrospray emitter and the MS orifice. By reversing the polarity, namely by grounding the emitter and applying the high potential to the counter electrode or the MS orifice, the required potential difference can also be achieved. This configuration, which is, for example, also used in MS instruments from Agilent or Bruker, was mimicked in the microscope setup by applying a negative voltage at the counter electrode, while the emitter was grounded. With this configuration, it was also possible to generate a stable intermitting electrospray at the tip. Video microscopic studies revealed that in this case, the droplet formation was unaffected by the electrical field for ESI generation, as shown in Fig. 3c. A droplet mass trace of an electrospray generated by this polarity

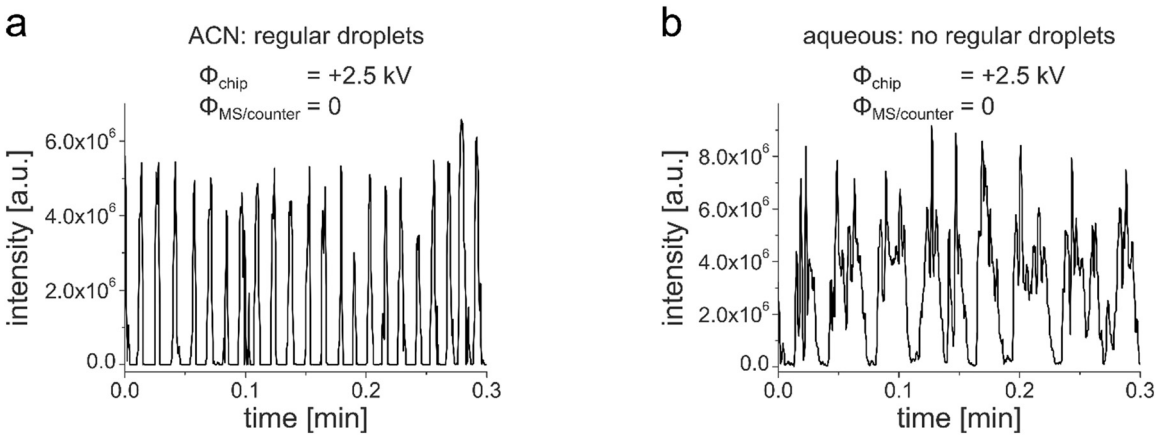

Fig. 2 Mass traces of on-chip generated droplets with electrical potential applied to the electrode on the chip and MS potential on ground for ESI(+). (a) ACN droplets show a regular and stable signal. (b) Aqueous droplets consisting of 10 mM NH_4OAc buffer at pH 7.4 show an irregular response.

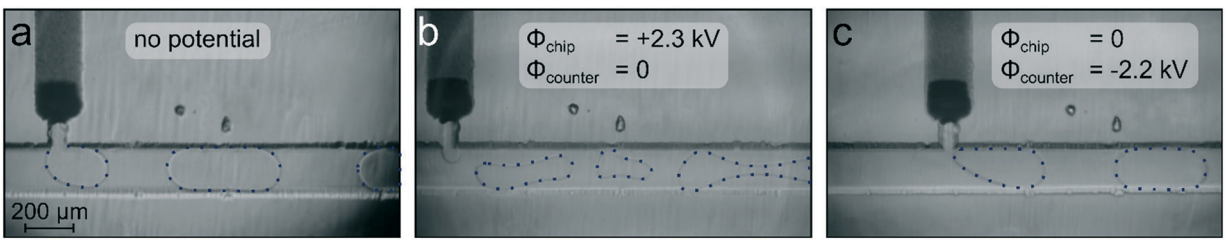

Fig. 3 Microscopic photographs of the droplet generation with different potentials Φ to form an electrospray at the emitter tip. (a) Droplet generation without applied potential. (b) The potential applied at the chip leads to irregular droplet generation. (c) The potential is applied at the counter electrode and the chip is grounded, which leads to no influence on the droplets. For better visualization, the droplets were highlighted by dotted lines.

configuration is shown in Fig. S2.† This finding that the impact of the electric field on droplet generation depends on the supply polarity as well as on the solvent composition of the dispersed phase was investigated in more detail.

The effect of the electrical potential on the droplets can be explained by electrowetting since the wetting properties of the droplet phase are changed by an applied electric field. The behavior of the droplets for the different applied potentials shown in Fig. 3 can be described qualitatively by the Lippmann–Young equation (eqn (1) in the ESI†).[61,62] This describes the change of the contact angle θ and the wetting properties $\cos\theta$ depending on the applied electrical potential. For a detailed description and interpretation, see chapter 4 and Fig. S3 in the ESI.† In brief, for a high electrical potential, $\cos\theta$ increases; it follows that the contact angle θ decreases. Therefore the droplets wet a larger area and change their shape.

An electrolyte concentration of 10 mM was chosen because preliminary experiments showed that at higher concentrations, the performance of electrospray ionization could suffer, for example, due to ion suppression. By varying the MeOH content from 30% to 50% (v/v), the electrolyte concentration also changed from 7 mM to 5 mM NH_4OAc. Since no different effects could be observed, the electrolyte concentration seems to play a minor role in the wetting effects. Therefore, further measurements were carried out with water instead of the electrolyte. The fact that the droplets were strongly influenced by the electric field for all mixtures with MeOH from 20% to 70% water content, as well as pure water, shows that the electric conductivity of the water is sufficient to cause the electrowetting effects, which lead to the destruction of the regular droplets. Only with electrolyte-free phases with extremely low conductivity, which consist of 100% acetonitrile or pure methanol, could a uniform segmented flow be achieved when applying a potential to the emitter (see Table S3†). Without an elevated electrical potential at the emitter tip, droplet generation was stable and regular in all cases studied.

As most ESI-MS instruments are designed in such a way that the emitter must be at elevated potential while the orifice is grounded, we investigated how to circumvent the observed droplet disruption in this configuration. An instrument with this source configuration, a Shimadzu quadrupole, was also intended for the experiments on droplet chip MS.

As a first approach to enable reliable chip-MS coupling with MS systems operating with a grounded orifice, shielding by attaching a grounded copper tape to the outside of the chip was investigated, following an approach which we utilized earlier in PDMS chips.[22,54] Therefore, copper strips were affixed at the top and the bottom of the chip in a T-shaped pattern shown in Fig. 4a and grounded. To leave free detection windows, the surface of the droplet channel was not entirely covered. With this setup, stable droplets could be successfully formed, as shown in Fig. 4b at the position of the droplet generator and in Fig. 4c at the location of the first detection window. At further downstream positions, however, droplet coalescence and increased wetting of the channel walls were observed (Fig. 4d). This behavior was also reproduced with other chips. Without applied potential, droplet generation and transport worked perfectly as always.

The experimental studies carried out revealed that the approach of electrical shielding seems promising, but the complete chip along the droplet channel should be covered by a conductive shield. At the same time, optical tracking of the droplets still should be possible. To address these requirements the chip was completely coated with a conductive and optical transparent indium tin oxide (ITO) layer except for the electrode and the tip (see photo in Fig. 5a).

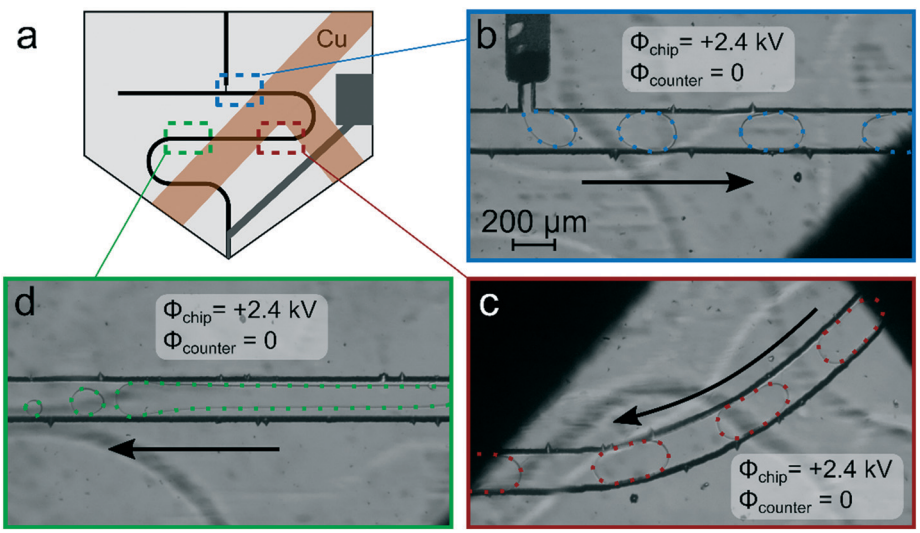

Fig. 4 (a) Schematic drawing of the microfluidic droplet chip with affixed grounded copper tape for shielding the electric field. (b) Despite an applied potential on-chip, the droplet formation works reliably and stably. (c) Even at further downstream positions in the channel, the droplets are still unaffected by the electrical field. (d) After passing the Cu tape, the droplet process becomes distorted again. Arrows mark the flow direction. For better visualization, the droplets were highlighted by dotted lines.

In the following measurements, however, no electrospray could be generated when the potential was applied to the platinum electrode while the ITO surface was grounded. Most likely there were conductive connections between the electrode and ITO, so that a sufficiently high potential difference between the chip and the counter electrode could not be formed. As the approach to use a grounded shield covering most of the chip in combination with a high potential at the emitter did not work reliably, the whole chip, namely the ITO coating and the emitter tip, were set on the same high potential. In this case, where potential gradients are avoided on the chip, the droplets showed regular and stable behaviour during droplet generation (Fig. 5b) and while flowing through the channel to the emitter tip (Fig. 5c).

This approach to just float the whole chip equipped with a conductive surface coating worked reliably, both in terms of stable droplet flow and electrospray ionization. However, in practice, it can be problematic if the whole chip is set to several kilovolts, and care has to be taken to avoid electrical flows to the peripherals such as the pumps and to ensure operational safety.

Another approach to preventing adverse effects of the electrospray potential at the emitter on the droplet flow and generation was to increase the distance between the emitter tip and the droplet generator.

For this purpose, we developed other chip designs to circumvent this problem. The approach of using a 4.8× longer droplet channel while the straight distance of droplet generator to the tip emitter remained unaffected, however, did not work. With this chip layout shown in Fig. S4,† a similar negative influence of electrical potentials on the droplets was observed.

However, with a new chip layout where we had the droplet generator as far away as possible from the chip tip, it finally worked. The finally functioning chip layout is shown in Fig. 6a. While all basic features were retained, their arrangement was changed. The column inlet was placed closer to the emitter with a flow direction away from the emitter. The droplet generator was located on the other side of the chip with the largest possible distance to the emitter tip and the electrode. This distancing approach did not affect the LC performance; the backpressure created by the packed column is very similar for both chip designs.

In this chip layout, we also enlarged the integrated electrode so that the platinum extended over the entire droplet channel width and beyond in order to increase the electrode robustness. With such microfluidic chips, it was now possible to form stable droplets and to guide them through the chip to the electrospray emitter, even when relatively high potentials of +4.0 kV were applied at the platinum electrode (Fig. 6b and c).

Hyphenating those chips to an MS instrument according to the arrangement described above allowed recording reliable and stable mass traces of the droplets, regardless of the potential configuration of the MS detector. Fig. 7a shows a characteristic periodic droplet response with a constant frequency of 0.7 Hz and intensity maxima of 3.1×10^6 counts with a relative standard deviation of 2.3%. With this setup, repetitive measurements could be performed over several hours. Additional videos show the process of droplet electrospray generation, which is periodically interrupted by the oil flow (Video S2†). The oil phase is drained off at the hydrophobic tip and led away by the PTFE tape attached near

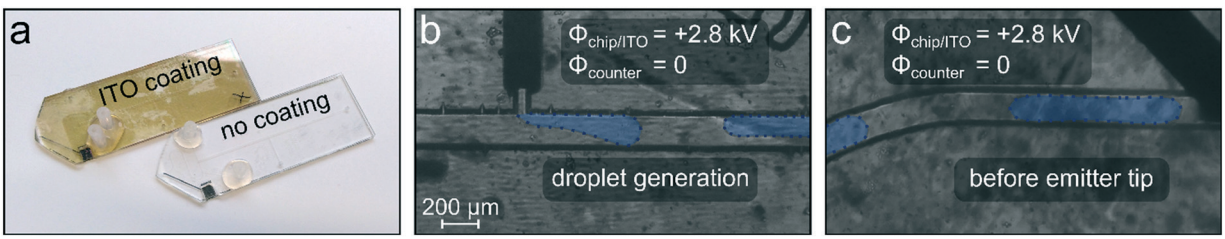

Fig. 5 (a) ITO-coated chip in comparison with a non-coated one. (b) Droplet formation worked reliably well and (c) they remained stable till they entered the emitter. 2.8 kV applied to the chip; counter electrode grounded. For better visualization, the droplets were highlighted in blue.

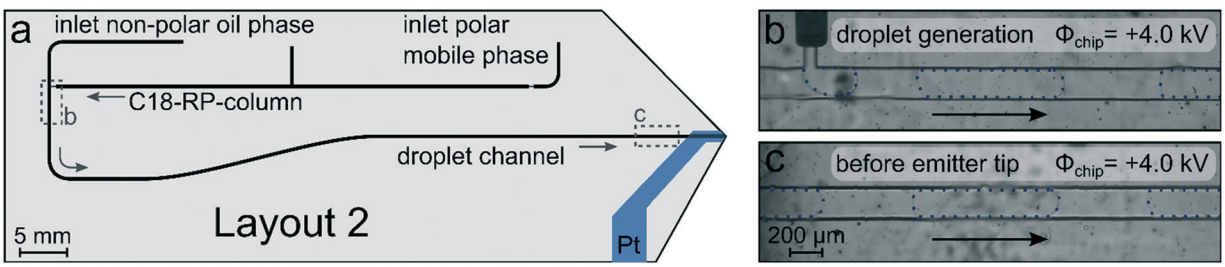

Fig. 6 (a) Schematic of chip layout 2 following the distancing approach. Flow directions are marked by arrows. (b) Droplet formation was reliably stable even at a high potential of 4.0 kV. (c) Droplets remain stable till they enter the emitter tip. For better visualization, the droplets were highlighted by dotted lines.

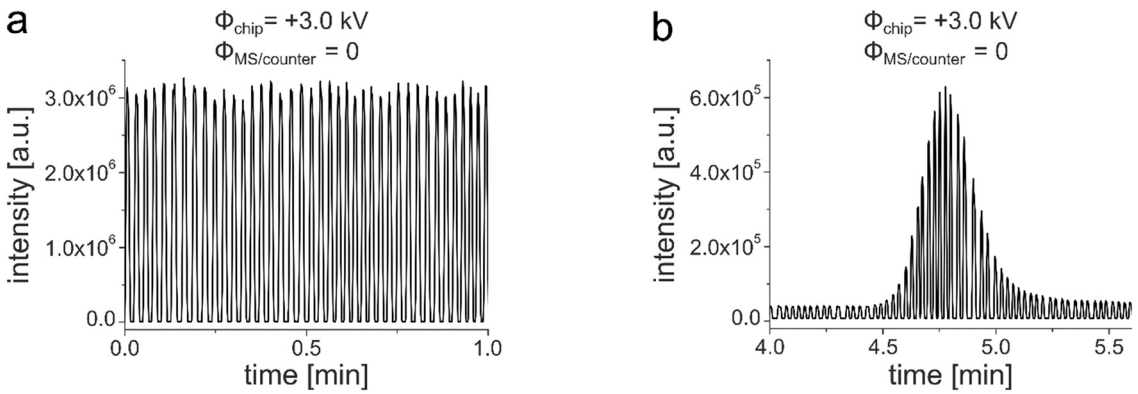

Fig. 7 (a) Mass trace of droplets generated on-chip with an electric potential applied to the chip electrode while the counter electrode and the MS inlet are grounded. (b) Mass trace of the compound 7-amino-4-methylcoumarin eluting from the column and segmented in droplets.

the emitter tip (Video S3†). After we were finally able to generate eluent droplets on the droplet/MS glass chip unaffected by the electrospray potentials, we tried to monitor a droplet segmented chromatographic peak eluting from the integrated LC column. For this purpose, 5 nL of the analyte (50 μM 7-amino-4-methylcoumarin in MeOH/H_2O 65/35 v/v) was injected *via* an external nano-valve. The HPLC eluent was pumped through the column at a flow rate of 0.5 μL min^{-1} applying 95 bar. After elution *via* the column, the peak was divided into individual segments by the oil phase. The typical Gaussian shape was retained but subdivided by the individual droplets (Fig. 7b).

Conclusion

On the way to developing a system for mass spectrometric detection of on-chip generated droplets, we hit on the phenomenon that droplets can be strongly influenced by high ESI potentials applied to the chip emitter. On closer examination, it became apparent that especially aqueous droplets were affected in their formation and transport, which can be explained by electrowetting effects. Different shielding approaches were investigated to decouple the droplets from the electric field. In particular, flooding of the entire chip to high voltage has proven to be very effective. The first HPLC-droplet/ESI-MS chip was finally accomplished by maximizing the distance of the droplet generator from the emitter. In this way, the microdroplets could be precisely transferred into an electrospray and detected by mass spectrometry. The segmentation of the chromatographic peak by oil spacers avoids diffusion and by that, peak dispersion. The narrow peak shape of a chromatographic peak can thus be maintained even during very long process times, *e.g.* in stop-flow mode or during storage. This now allows post column processing of the chromatographically separated components by using the powerful droplet microfluidics toolbox. Especially interesting are post-column reactions of the purified substrates, *e.g.* for enzyme assays[63] with MS detection.[64]

Conflicts of interest

There are no conflicts to declare.

Acknowledgements

This work was funded by the Deutsche Forschungsgemeinschaft (DFG, German Research Foundation) FOR 2177, BE 1922/12-2. We would like to thank Marina Heinrich for her support with the chip production.

References

1 Y. Ding, P. D. Howes and A. J. deMello, Recent Advances in Droplet Microfluidics, *Anal. Chem.*, 2020, **92**, 132–149.
2 Y. Geng, S. Ling, J. Huang and J. Xu, Multiphase Microfluidics: Fundamentals, Fabrication, and Functions, *Small*, 2020, **16**, e1906357.
3 Y. Ai, R. Xie, J. Xiong and Q. Liang, Microfluidics for Biosynthesizing: from Droplets and Vesicles to Artificial Cells, *Small*, 2020, **16**, e1903940.
4 H. Feng, T. Zheng, M. Li, J. Wu, H. Ji, J. Zhang, W. Zhao and J. Guo, Droplet-based microfluidics systems in biomedical applications, *Electrophoresis*, 2019, **40**, 1580–1590.
5 A. Autour and M. Ryckelynck, Ultrahigh-Throughput Improvement and Discovery of Enzymes Using Droplet-Based Microfluidic Screening, *Micromachines*, 2017, **8**, 128.
6 D. Hümmer, F. Kurth, N. Naredi-Rainer and P. S. Dittrich, Single cells in confined volumes: microchambers and microdroplets, *Lab Chip*, 2016, **16**, 447–458.
7 E. E. Kempa, K. A. Hollywood, C. A. Smith and P. E. Barran, High throughput screening of complex biological samples with mass spectrometry - from bulk measurements to single cell analysis, *Analyst*, 2019, **144**, 872–891.
8 F. Pereira, X. Niu and A. J. deMello, A nano LC-MALDI mass spectrometry droplet interface for the analysis of complex protein samples, *PLoS One*, 2013, **8**, e63087.
9 S. K. Küster, M. Pabst, K. Jefimovs, R. Zenobi and P. S. Dittrich, High-resolution droplet-based fractionation of nano-LC separations onto microarrays for MALDI-MS analysis, *Anal. Chem.*, 2014, **86**, 4848–4855.

10 D. Haidas, M. Napiorkowska, S. Schmitt and P. S. Dittrich, Parallel Sampling of Nanoliter Droplet Arrays for Noninvasive Protein Analysis in Discrete Yeast Cultivations by MALDI-MS, *Anal. Chem.*, 2020, **92**, 3810–3818.
11 J. Pei, Q. Li, M. S. Lee, G. A. Valaskovic and R. T. Kennedy, Analysis of samples stored as individual plugs in a capillary by electrospray ionization mass spectrometry, *Anal. Chem.*, 2009, **81**, 6558–6561.
12 Q. Li, J. Pei, P. Song and R. T. Kennedy, Fraction Collection from Capillary Liquid Chromatography and Off-line Electrospray Ionization Mass Spectrometry Using Oil Segmented Flow, *Anal. Chem.*, 2010, **82**, 5260–5267.
13 S. Sun, T. R. Slaney and R. T. Kennedy, Label free screening of enzyme inhibitors at femtomole scale using segmented flow electrospray ionization mass spectrometry, *Anal. Chem.*, 2012, **84**, 5794–5800.
14 S. Sun and R. T. Kennedy, Droplet electrospray ionization mass spectrometry for high throughput screening for enzyme inhibitors, *Anal. Chem.*, 2014, **86**, 9309–9314.
15 S. Sun, B. C. Buer, E. N. G. Marsh and R. T. Kennedy, A label-free Sirtuin 1 assay based on droplet-electrospray ionization mass spectrometry, *Anal. Methods*, 2016, **8**, 3458–3465.
16 X. W. Diefenbach, I. Farasat, E. D. Guetschow, C. J. Welch, R. T. Kennedy, S. Sun and J. C. Moore, Enabling Biocatalysis by High-Throughput Protein Engineering Using Droplet Microfluidics Coupled to Mass Spectrometry, *ACS Omega*, 2018, **3**, 1498–1508.
17 D. J. Steyer and R. T. Kennedy, High-Throughput Nanoelectrospray Ionization-Mass Spectrometry Analysis of Microfluidic Droplet Samples, *Anal. Chem.*, 2019, **91**, 6645–6651.
18 J. Ji, L. Nie, L. Qiao, Y. Li, L. Guo, B. Liu, P. Yang and H. H. Girault, Proteolysis in microfluidic droplets: an approach to interface protein separation and peptide mass spectrometry, *Lab Chip*, 2012, **12**, 2625–2629.
19 J. Ji, L. Nie, Y. Li, P. Yang and B. Liu, Simultaneous online enrichment and identification of trace species based on microfluidic droplets, *Anal. Chem.*, 2013, **85**, 9617–9622.
20 C. A. Smith, X. Li, T. H. Mize, T. D. Sharpe, E. I. Graziani, C. Abell and W. T. S. Huck, Sensitive, high throughput detection of proteins in individual, surfactant-stabilized picoliter droplets using nanoelectrospray ionization mass spectrometry, *Anal. Chem.*, 2013, **85**, 3812–3816.
21 R. J. Beulig, R. Warias, J. J. Heiland, S. Ohla, K. Zeitler and D. Belder, A droplet-chip/mass spectrometry approach to study organic synthesis at nanoliter scale, *Lab Chip*, 2017, **17**, 1996–2002.
22 K. Wink, L. Mahler, R. J. Beulig, S. K. Piendl, M. Roth and D. Belder, An integrated chip-mass spectrometry and epi-fluorescence approach for online monitoring of bioactive metabolites from incubated Actinobacteria in picoliter droplets, *Anal. Bioanal. Chem.*, 2018, **410**, 7679–7687.
23 R. F. Gerhardt, A. J. Peretzki, S. K. Piendl and D. Belder, Seamless Combination of High-Pressure Chip-HPLC and Droplet Microfluidics on an Integrated Microfluidic Glass Chip, *Anal. Chem.*, 2017, **89**, 13030–13037.
24 A. J. Peretzki and D. Belder, On-chip integration of normal phase high-performance liquid chromatography and droplet microfluidics introducing ethylene glycol as polar continuous phase for the compartmentalization of n-heptane eluents, *J. Chromatogr. A*, 2020, **1612**, 460653.
25 J.-Y. Kim, S.-W. Cho, D.-K. Kang, J. B. Edel, S.-I. Chang, A. J. deMello and D. O'Hare, Lab-chip HPLC with integrated droplet-based microfluidics for separation and high frequency compartmentalisation, *Chem. Commun.*, 2012, **48**, 9144–9146.
26 J.-Y. Kim, S.-I. Chang, A. J. deMello and D. O'Hare, Integration of monolithic porous polymer with droplet-based microfluidics on a chip for nano/picoliter volume sample analysis, *Nano Convergence*, 2014, **1**, 368.
27 H. Song, D. L. Chen and R. F. Ismagilov, Reactions in droplets in microfluidic channels, *Angew. Chem., Int. Ed.*, 2006, **45**, 7336–7356.
28 A. J. deMello, Control and detection of chemical reactions in microfluidic systems, *Nature*, 2006, **442**, 394–402.
29 A. Huebner, S. Sharma, M. Srisa-Art, F. Hollfelder, J. B. Edel and A. J. deMello, Microdroplets: a sea of applications?, *Lab Chip*, 2008, **8**, 1244–1254.
30 A. K. Price and B. M. Paegel, Discovery in Droplets, *Anal. Chem.*, 2016, **88**, 339–353.
31 S. Mashaghi, A. Abbaspourrad, D. A. Weitz and A. M. van Oijen, Droplet microfluidics: A tool for biology, chemistry and nanotechnology, *TrAC, Trends Anal. Chem.*, 2016, **82**, 118–125.
32 M. Joanicot and A. Ajdari, Droplet control for microfluidics, *Science*, 2005, **309**, 887–888.
33 S. Xu, Z. Nie, M. Seo, P. Lewis, E. Kumacheva, H. A. Stone, P. Garstecki, D. B. Weibel, I. Gitlin and G. M. Whitesides, Generation of Monodisperse Particles by Using Microfluidics: Control over Size, Shape, and Composition, *Am. Ethnol.*, 2005, **117**, 734–738.
34 V. Trivedi, A. Doshi, G. K. Kurup, E. Ereifej, P. J. Vandevord and A. S. Basu, A modular approach for the generation, storage, mixing, and detection of droplet libraries for high throughput screening, *Lab Chip*, 2010, **10**, 2433–2442.
35 C.-G. Yang, Z.-R. Xu and J.-H. Wang, Manipulation of droplets in microfluidic systems, *TrAC, Trends Anal. Chem.*, 2010, **29**, 141–157.
36 A. G. Chambers, J. S. Mellors, W. H. Henley and J. M. Ramsey, Monolithic integration of two-dimensional liquid chromatography-capillary electrophoresis and electrospray ionization on a microfluidic device, *Anal. Chem.*, 2011, **83**, 842–849.
37 Y. Zhu and Q. Fang, Integrated droplet analysis system with electrospray ionization-mass spectrometry using a hydrophilic tongue-based droplet extraction interface, *Anal. Chem.*, 2010, **82**, 8361–8366.
38 C. Lotter, J. J. Heiland, S. Thürmann, L. Mauritz and D. Belder, HPLC-MS with Glass Chips Featuring Monolithically Integrated Electrospray Emitters of Different Geometries, *Anal. Chem.*, 2016, **88**, 2856–2863.
39 C. Lotter, J. J. Heiland, V. Stein, M. Klimkait, M. Queisser and D. Belder, Evaluation of Pressure Stable Chip-to-Tube

Fittings Enabling High-Speed Chip-HPLC with Mass Spectrometric Detection, *Anal. Chem.*, 2016, **88**, 7481–7486.
40 D. R. Link, E. Grasland-Mongrain, A. Duri, F. Sarrazin, Z. Cheng, G. Cristobal, M. Marquez and D. A. Weitz, Electric control of droplets in microfluidic devices, *Angew. Chem., Int. Ed.*, 2006, **45**, 2556–2560.
41 Z. Z. Chong, S. H. Tan, A. M. Gañán-Calvo, S. B. Tor, N. H. Loh and N.-T. Nguyen, Active droplet generation in microfluidics, *Lab Chip*, 2016, **16**, 35–58.
42 M. Chabert, K. D. Dorfman and J.-L. Viovy, Droplet fusion by alternating current (AC) field electrocoalescence in microchannels, *Electrophoresis*, 2005, **26**, 3706–3715.
43 M. Zagnoni and J. M. Cooper, On-chip electrocoalescence of microdroplets as a function of voltage, frequency and droplet size, *Lab Chip*, 2009, **9**, 2652–2658.
44 R. He, M. Ruan, Y. Qi, H. Liu, Z. Zhang, C. Chen, Y. Chao, Y. Liu and Y. Chen, Engineering of Droplet Charges in Microfluidic Chips, *Adv. Eng. Mater.*, 2020, **22**, 1901521.
45 L. M. Fidalgo, G. Whyte, D. Bratton, C. F. Kaminski, C. Abell and W. T. S. Huck, From microdroplets to microfluidics: selective emulsion separation in microfluidic devices, *Angew. Chem., Int. Ed.*, 2008, **47**, 2042–2045.
46 L. M. Fidalgo, G. Whyte, B. T. Ruotolo, J. L. P. Benesch, F. Stengel, C. Abell, C. V. Robinson and W. T. S. Huck, Coupling microdroplet microreactors with mass spectrometry: reading the contents of single droplets online, *Angew. Chem., Int. Ed.*, 2009, **48**, 3665–3668.
47 M. Girault, H. Kim, H. Arakawa, K. Matsuura, M. Odaka, A. Hattori, H. Terazono and K. Yasuda, An on-chip imaging droplet-sorting system: a real-time shape recognition method to screen target cells in droplets with single cell resolution, *Sci. Rep.*, 2017, **7**, 40072.
48 H.-D. Xi, H. Zheng, W. Guo, A. M. Gañán-Calvo, Y. Ai, C.-W. Tsao, J. Zhou, W. Li, Y. Huang, N.-T. Nguyen and S. H. Tan, Active droplet sorting in microfluidics: a review, *Lab Chip*, 2017, **17**, 751–771.
49 S. Hasan, D. Geissler, K. Wink, A. Hagen, J. J. Heiland and D. Belder, Fluorescence lifetime-activated droplet sorting in microfluidic chip systems, *Lab Chip*, 2019, **19**, 403–409.
50 I. Barbulovic-Nad, H. Yang, P. S. Park and A. R. Wheeler, Digital microfluidics for cell-based assays, *Lab Chip*, 2008, **8**, 519–526.
51 J. Lee, H. Moon, J. Fowler, T. Schoellhammer and C.-J. Kim, Electrowetting and electrowetting-on-dielectric for microscale liquid handling, *Sens. Actuators, A*, 2002, **95**, 259–268.
52 M. G. Pollack, R. B. Fair and A. D. Shenderov, Electrowetting-based actuation of liquid droplets for microfluidic applications, *Appl. Phys. Lett.*, 2000, **77**, 1725–1726.
53 A. R. Wheeler, H. Moon, C.-J. Kim, J. A. Loo and R. L. Garrell, Electrowetting-based microfluidics for analysis of peptides and proteins by matrix-assisted laser desorption/ionization mass spectrometry, *Anal. Chem.*, 2004, **76**, 4833–4838.
54 M. Schirmer, K. Wink, S. Ohla, D. Belder, A. Schmid and C. Dusny, Conversion Efficiencies of a Few Living Microbial Cells Detected at a High Throughput by Droplet-Based ESI-MS, *Anal. Chem.*, 2020, **92**(15), 10700–10708.
55 S. Thürmann, L. Mauritz, C. Heck and D. Belder, High-performance liquid chromatography on glass chips using precisely defined porous polymer monoliths as particle retaining elements, *J. Chromatogr. A*, 2014, **1370**, 33–39.
56 P. Hoffmann, U. Häusig, P. Schulze and D. Belder, Microfluidic Glass Chips with an Integrated Nanospray Emitter for Coupling to a Mass Spectrometer, *Angew. Chem., Int. Ed.*, 2007, **46**, 4913–4916.
57 S. Fritzsche, S. Ohla, P. Glaser, D. S. Giera, M. Sickert, C. Schneider and D. Belder, Asymmetric organocatalysis and analysis on a single microfluidic nanospray chip, *Angew. Chem., Int. Ed.*, 2011, **50**, 9467–9470.
58 C. Dietze, C. Hackl, R. F. Gerhardt, S. Seim and D. Belder, Chip-based electrochromatography coupled to ESI-MS detection, *Electrophoresis*, 2016, **37**, 1345–1352.
59 M. Pahl, M. Mayer, M. Schneider, D. Belder and K. R. Asmis, Joining Microfluidics with Infrared Photodissociation: Online Monitoring of Isomeric Flow-Reaction Intermediates, *Anal. Chem.*, 2019, **91**, 3199–3203.
60 P. Song, N. D. Hershey, O. S. Mabrouk, T. R. Slaney and R. T. Kennedy, Mass spectrometry "sensor" for in vivo acetylcholine monitoring, *Anal. Chem.*, 2012, **84**, 4659–4664.
61 M. G. Lippmann, Relations entre les phénomènes électriques et capillaires, *Ann. Chim. Phys.*, 1875, **5**, 494.
62 T. Young, III, An essay on the cohesion of fluids, *Philos. Trans. R. Soc. London*, 1805, **95**, 65–87.
63 A. Ochoa, E. Álvarez-Bohórquez, E. Castillero and L. F. Olguin, Detection of Enzyme Inhibitors in Crude Natural Extracts Using Droplet-Based Microfluidics Coupled to HPLC, *Anal. Chem.*, 2017, **89**, 4889–4896.
64 Y. Yuan, M. Zhao, L. Riffault-Valois, S. Ennahar, M. Bergaentzlé and E. Marchioni, Online acetylcholinesterase inhibition evaluation by high-performance liquid chromatography–mass spectrometry hyphenated with an immobilized enzyme reactor, *J. Chromatogr. A*, 2020, **1609**, 460506.